

Evolution of Natural Myocardial Shear Wave Behavior in Young Hearts: Determinant Factors and Reproducibility Analysis



Ahmed S. Youssef, MD, Aniela Petrescu, MD, PhD, Thomas Salaets, MD, Stéphanie Bézy, MSc, PhD, Laurine Wouters, MSc, Marta Orłowska, MSc, PhD, Annette Caenen, MSc, PhD, Jürgen Duchenne, MSc, PhD, Alexis Puvrez, MD, Bjorn Cools, MD, PhD, Ruth Heying, MD, PhD, Jan D'hooge, MSc, PhD, Marc Gewillig, MD, PhD, and Jens-Uwe Voigt, MD, PhD, *Leuven and Ghent, Belgium; Ismailia, Egypt; and Mainz, Germany*

Background: Myocardial diastolic function assessment in children by conventional echocardiography is challenging. High-frame rate echocardiography facilitates the assessment of myocardial stiffness, a key factor in diastolic function, by measuring the propagation velocities of myocardial shear waves (SWs). However, normal values of natural SWs in children are currently lacking. The aim of this study was to explore the behavior of natural SWs among children and adolescents, their reproducibility, and the factors affecting SW velocities from childhood into adulthood.

Methods: One hundred six healthy children (2-18 years of age) and 62 adults (19-80 years of age) were recruited. High-frame rate images were acquired using a modified commercial scanner. An anatomic M-mode line was drawn along the ventricular septum, and propagation velocities of natural SWs after mitral valve closure were measured in the tissue acceleration-coded M-mode display.

Results: Throughout life, SW velocities after mitral valve closure exhibited pronounced age dependency ($r = 0.73$; $P < .001$). Among the pediatric population, SW velocities correlated significantly with measures of cardiac geometry (septal thickness and left ventricular end-diastolic dimension), local hemodynamics (systolic blood pressure), and echocardiographic parameters of systolic and diastolic function (global longitudinal strain, mitral E/e' ratio, isovolumic relaxation time, and mitral deceleration time) ($P < .001$). In a multivariate analysis including all these factors, the predictors of SW velocities were age, mitral E/e', and global longitudinal strain ($r = 0.81$).

Conclusions: Natural myocardial SW velocities in children can be detected and measured. SW velocities showed significant dependence on age and diastolic function. Natural SWs could be a promising additive tool for the assessment of diastolic function among children. (*J Am Soc Echocardiogr* 2024;37:1051-61.)

Keywords: Natural shear waves, Echocardiography, High frame rate, Myocardial stiffness, Pediatric diastolic function

Diastolic function assessment in a pediatric population with diverse cardiac problems, whether congenital or acquired, is crucial for understanding symptoms and guiding treatment.¹ Diastolic dysfunction could be the earliest pathologic change in symptomatic children

despite normal systolic heart function. Therefore, a thorough assessment of diastolic function in children holds prognostic implications.² Nevertheless, current echocardiographic parameters are limited by variations in cardiac geometry (heart size) and hemodynamics (heart

From the Department of Cardiovascular Sciences, KU Leuven, Leuven, Belgium (A.S.Y., A.P., S.B., L.W., M.O., A.C., J. Duchenne, A.P., B.C., R.H., J. D'hooge, M.G., J.-U.V.); the Department of Cardiovascular Medicine, Suez Canal University, Ismailia, Egypt (A.S.Y.); the Department of Cardiology, University Medical Center of the Johannes Gutenberg-Universität Mainz, Mainz, Germany (A.P.); the Department of Pediatric Cardiology, University Hospitals Leuven, Leuven, Belgium (T.S., B.C., R.H., M.G.); the Department of Electronics and Information Systems, Ghent University, Ghent, Belgium (A.C.); and the Department of Cardiovascular Diseases, University Hospitals Leuven, Leuven, Belgium (J.-U.V.).

Dr. Youssef is supported by a scholarship from the Egyptian Ministry of Research and Higher Education (2021 recipient) and by the Belgian Fund for Cardiac Surgery

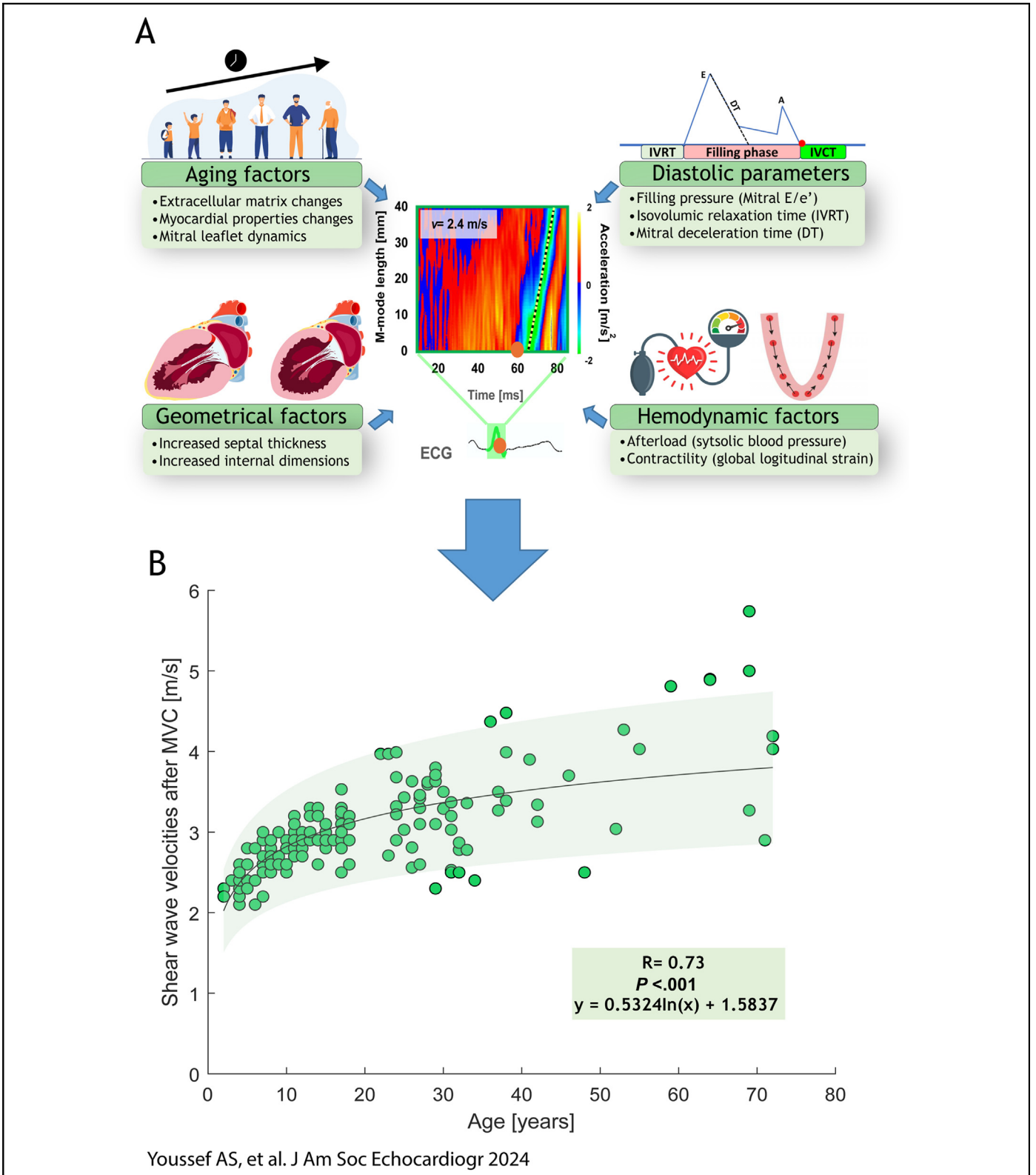
(489708). Dr. Salaets is supported by the Frans Van de Werf Fund for Clinical Cardiovascular Research (2022 recipient), by De Kleine Hartjes VZW, and by the Research Foundation Flanders (V401622 N). Drs. Caenen, Heying, Jürgen Duchenne, and Voigt hold a personal research mandate of the Research Foundation Flanders (1211620N, 1881820N, 12ZZN22N, and 1832922N respectively).

Reprint requests: Jens-Uwe Voigt, MD, PhD, Department of Cardiovascular Diseases, University Hospitals Leuven, Herestraat 49, 3000 Leuven, Belgium (E-mail: jens-uwe.voigt@uzleuven.be).

0894-7317/\$36.00

Copyright 2024 by the American Society of Echocardiography.

<https://doi.org/10.1016/j.echo.2024.07.004>



Central Illustration (A) Factors affecting the behavior of natural SWs in the pediatric population. **(B)** SW velocities as a function of age. A logarithmic regression model with its 95% CI was fitted to the data, taking the heteroscedasticity of the data into account for the error model. The Pearson correlation coefficient (r) was calculated to quantify the strength and direction of the relationship between SW velocities and age. ECG, Electrocardiogram; IVCT, isovolumic contraction time.

Abbreviations
ARF = Acoustic radiation force
DT = Deceleration time
GLS = Global longitudinal strain
HFR = High-frame rate
ICC = Intraclass correlation coefficient
IVRT = Isovolumic relaxation time
IVS = Interventricular septum
LV = Left ventricular
LVEDD = Left ventricular end-diastolic diameter
MS = Myocardial stiffness
MVC = Mitral valve closure
SBP = Systolic blood pressure
SW = Shear wave
SWE = Shear wave elastography

rate and loading conditions) during childhood,¹ leading to a broad range of normal values that might not effectively identify diastolic dysfunction.³

Cardiac diastole is a complex process that incorporates the interplay between active myocardial relaxation, left ventricular (LV) diastolic recoil, and passive myocardial stiffness (MS). These three determinants, modulated by LV geometry and loading conditions, determine the filling pressure of the LV, which in turn is used as clinical surrogate of diastolic function.⁴ LV filling pressures can be approximated by conventional echocardiography, but the approach has a wide error range and often detects only later stages of disease reliably.⁵ Importantly, these approximations have never been validated in children. Therefore, the adoption of a more precise, clinically feasible, noninvasive tool capable of identifying diastolic

dysfunction is desirable. This is of particular importance in pediatric cardiac diseases, in which changes in MS are a hallmark pathologic finding (e.g., hypertrophic cardiomyopathy and post-Fontan palliation).^{6,7}

Recently, measuring the propagation velocity of shear waves (SWs) in the myocardium has been proposed for the assessment of MS, one of the key components of diastolic function.⁸ Nonetheless, conventional echocardiography has insufficient temporal resolution for tracking such short-lived fast-motion events.⁹ Recent developments in transducer design and processing power, however, allow diverging-wave imaging at up to 5,000 frames/sec, which is sufficient for capturing myocardial SWs.^{1,10} High-frame rate (HFR) imaging-based SW elastography (SWE) could therefore become a technically feasible innovative tool for the direct assessment of MS.^{11,12}

Myocardial SWs can be either externally induced by a strong ultrasound pulse (acoustic radiation force [ARF]) or naturally induced through a mechanical event (e.g., mitral valve closure [MVC]). Then, they propagate through the myocardium at a velocity that is directly linked to MS.¹¹ ARF-induced waves have a high frequency content and low amplitude, and they decay rapidly, which makes their detection and speed estimation challenging even in an echogenic pediatric population. Natural waves have a lower frequency content and higher amplitude, and they attenuate less during propagation. This improves feasibility for SW detection and the accuracy of wave speed estimates.^{11,13,14} The timing of natural wave measurements is, however, restricted to the valve closure events (i.e., the beginning of the respective isovolumic intervals).^{12,15}

Natural SWE-derived MS has been validated in phantoms, animals, and humans^{16,17} and shown to provide clinically useful information in pathology in adults.¹⁸⁻²¹ SW elastographic studies in children have so far been focused mainly on the behavior of ARF-induced SWs^{6,22} and have reported a linear correlation between SW velocities at end-

diastole with age and the geometric characteristics of the left ventricle.²³ Reports of normal values of natural SWs in children, however, remain scarce, and systematic data about their changes during childhood and adolescence are lacking.^{15,22,24}

In our study, we explored natural SW velocities in a large group of children and adolescents with the aim of developing a normal reference range from childhood into adulthood as a step toward implementing this novel parameter in clinical practice. We also aimed to determine the variability of our measurements and to explore the factors that might influence SW velocity estimates in the growing hearts. For the latter aim, we compared both clinical data and results from computer modeling.

METHODS

Study Population

This was a single-center observational study conducted at the University Hospitals Leuven in Belgium. One hundred eight healthy volunteers 2 to 18 years of age were recruited through a public announcement. To explore the behavior of natural SWs with aging in adulthood, collected SW elastographic data were compared with acquisitions from 62 healthy adults 19 to 80 years of age. Some of the adult volunteers participated during this study, whereas others were recruited by Petrescu *et al.*¹⁹ in the context of a previous study. All data sets were analyzed by the same reader (A.Y.). Exclusion criteria were a history of cardiac abnormalities, a history of previous cardiac disease or cardiac risk factors (e.g., hypertension, diabetes), conduction abnormalities or arrhythmias other than occasional premature beats, and a history of previous systemic treatment with a potential effect on the heart (e.g., chemotherapy). Furthermore, patients with pathologic findings on conventional echocardiography or poor echogenicity were excluded.

All healthy volunteers underwent both conventional transthoracic echocardiography and HFR imaging for SWE. This study was approved by the ethics committee of the University Hospitals Leuven. Written informed consent was obtained from all participants 12 years and older as well as from the parents of all participants younger than 18 years.

Conventional Echocardiography

Conventional echocardiography was performed using an E95 scanner (GE Vingmed Ultrasound) equipped with a phased-array ultrasound probe (M5S-D). Parasternal and apical standard views as well as spectral and color Doppler data were acquired and stored as raw Digital Imaging and Communications in Medicine data. Offline analysis was performed using EchoPAC PC version 204 (GE Vingmed Ultrasound). We measured conventional parameters of LV morphology and systolic and diastolic function (LV dimensions, LV biplane ejection fraction, mitral annular velocity, and tissue Doppler parameters) as well as the average global longitudinal strain (GLS) from three planes (apical four-, two-, and three-chamber views). Z scores and percentiles were calculated where appropriate.²⁵

HFR Imaging

HFR image data were recorded using the same aforementioned scanner and the same probe after switching the operating mode from conventional scanning to diverging-wave imaging, in

HIGHLIGHTS

- Easy detection and trackability of pediatric cardiac natural SWs are demonstrated.
- Natural SWs showed clear dependence on age, implying increasing MS.
- Age-specific reference values for SWs are needed when assessing MS.
- SWs correlate well with parameters used to assess diastolic function in children.

which one echo impulse generates one image instead of one image line.^{1,8} Coherent compounding of four diverging-wave images resulted in an average frame rate of $1,295 \pm 164$ frames/sec. We acquired parasternal long-axis images for 3 sec. Raw data were digitally stored for further offline beamforming and reconstruction. Doppler processing was used to obtain tissue acceleration.

The timing of MVC was determined by visual assessment of valve closure or, if needed, on the basis of time-aligned pulsed-wave Doppler tracing. Then, an anatomic M-mode line was drawn from the base toward the apex along the midline of the interventricular septum (IVS) around the time of MVC. The M-mode display was color coded for tissue acceleration so that the propagation of SWs from base to apex became visible as a tilted green band, the slope of which was measured semiautomatically. For this, the clinician identified the approximate position of the wave of interest (the first wave immediately after MVC) with a mouse click, and then the slope of the wave was calculated as best fit to the automatically detected first acceleration nadir (Figure 1). The result was visually checked and manually adjusted, if needed.

All HFR image postprocessing and analysis were performed using in-house-developed MATLAB-based (The MathWorks) software (SPEQLE). A detailed description of data acquisition, processing, and SW analysis has been previously provided.^{13,18}

All SW velocity measurements were repeated three times by the same reader (A.Y.) and averaged. Measurement variability was evaluated at four levels:

- slope estimation reproducibility, in which the SW slope was reevaluated on the same anatomic M-mode line of the same image acquisition by the same observer (A.Y.);
- intraobserver variability, in which the same observer drew a new M-mode line on the same image acquisition and measured the slope of the SW;
- interobserver variability, in which another observer (L.W.), blinded to previous results, repeated drawing the M-mode line and measuring SW slopes in the same image acquisition; and
- test-retest variability, in which two subsequent image acquisitions, taken during the same examination without any modifications in image settings, were analyzed for SW velocities by the same observer.

Simulation Model for SW Propagation in the Heart

To study the potential effects of geometric changes of a growing heart, we evaluated SW propagation velocities in relation to wall thickness in a theoretical wave propagation model. In the model, the myocardial wall was approximated as a linear elastic plate loaded with fluids on both sides (Lamb wave model^{26,27}). As no exact analytic solutions are available, a discrete numeric solution was calculated using MATLAB R2023a. We focused on the first-order antisymmetric wave mode, which is the dominant wave mode with shear motion at low frequencies, similar to natural SWs. Plate stiffness was set to 350 kPa in the model to obtain a wave propagation speed of 3.2 m/sec at a wave frequency of 50 Hz, which has been reported as the dominant frequency of SWs after MVC²⁸ in healthy volunteers with a wall thickness of 10 mm.¹⁸ To study the effect of wall thickness on propagation speed, the wall thickness was varied from 0.5 to 20 mm (Figure 2A).

Statistical Analysis

First, data normality was checked using the Shapiro-Wilk test. Continuous data are presented as mean \pm SD, and categorical data

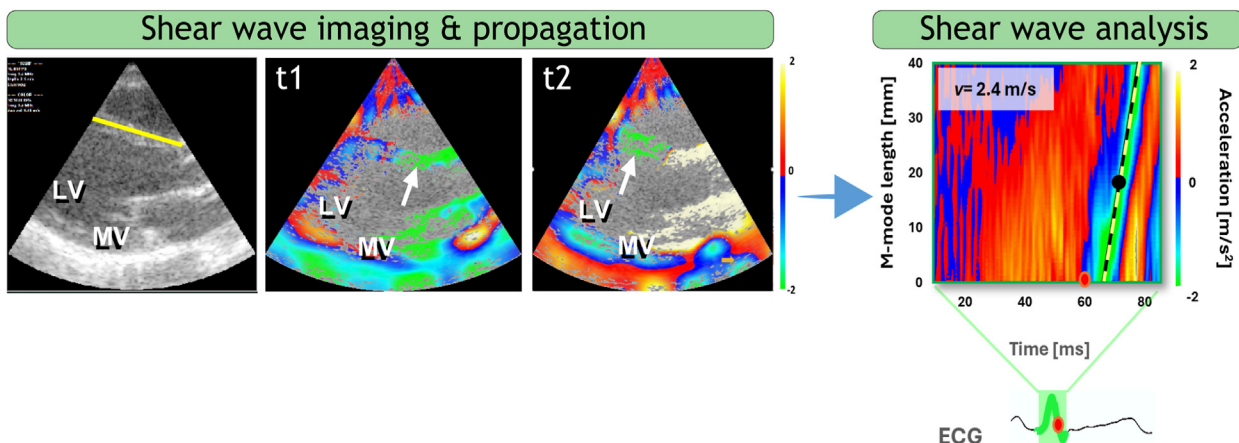


Figure 1 SW imaging and processing. On the B-mode image, an anatomic M-mode line is drawn along the septum (left). Tissue Doppler acceleration shows a SW propagating from base to apex (indicated by white arrows at two time points, t1 and t2). In the M-mode image, the SW becomes visible as a tilted green band starting after MVC (red dot). The clinician identifies the wave of interest by a mouse click (black dot), and its slope (black/yellow dotted line), representing the propagation velocity (v), is then determined automatically. The highlighted portion of the electrocardiogram (ECG) corresponds to the time interval displayed in the M-mode image, and the red dot represents the onset of the SW on the ECG. LV, Left ventricle; MV, mitral valve.

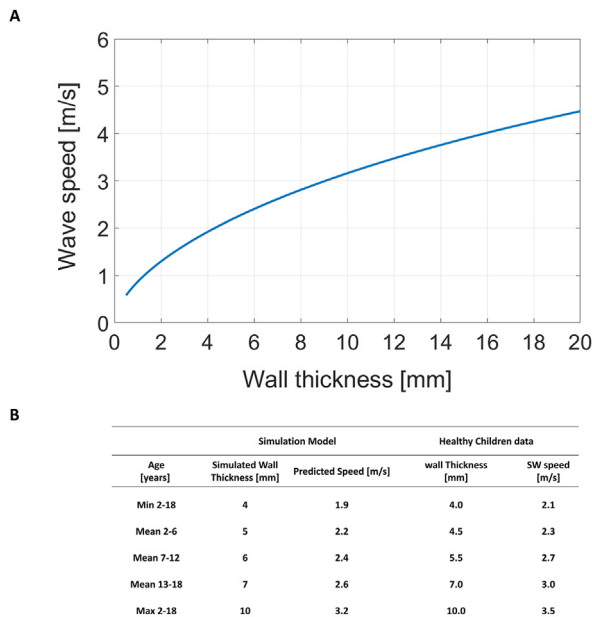


Figure 2 Modeling of SW velocities in a fluid-loaded plate: Lamb wave theory. **(A)** Our theoretical wave propagation model showed a clear increase in SW propagation speed at 50 Hz (the dominant frequency of SWs after MVC) when the wall thickness increases, as observed in our *in vivo* study. **(B)** Model results were compared with observed wall thicknesses and respective SW velocities in our group of young healthy volunteers. In the model, the myocardial wall was approximated as a linear elastic plate loaded with fluids on both sides. Plate stiffness was set to 350 kPa. We focused on a wave frequency of 50 Hz, which is the dominant frequency of SWs after MVC. *Max*, Maximum; *min*, minimum.

are reported as frequencies and percentages. A univariate linear regression model was used. Pearson correlation coefficients were calculated to identify the pairwise correlations between SW velocity and demographic variables (e.g., age), clinical data (e.g., systolic blood pressure [SBP], diastolic blood pressure), echocardiographic parameters (e.g., IVS thickness, LV end-diastolic diameter [LVEDD], LV end-diastolic volume), and conventional echocardiographic parameters of diastolic function (e.g., mitral E/e' ratio, isovolumic relaxation time [IVRT], and deceleration time [DT]).

Subsequently, all significant variables were included in a backward multivariate linear regression model to identify the potential predictors of natural SW velocities. Analysis of variance was conducted using *F* statistics and *P* values to assess how well the regression model fit the data. To control for the number of covariates, a *P* value $\geq .10$ was set as the threshold for removal. Collinearity diagnostics were performed and *Z* scores were used when needed. After that, a curve estimation was performed in which the logarithmic regression model was the best-fit model for the relationship between age and SW velocities.

Finally, slope estimation, intraobserver, interobserver (between the two observers, A.Y. and L.W.), and test-retest variabilities were evaluated in 25 randomly selected young healthy volunteers using the intraclass correlation coefficient (ICC; two-way mixed model, absolute agreement between single measures). Moreover, Bland-Altman analysis was performed to assess reproducibility. All statistical analyses were done in SPSS version 24.0 (IBM), and a two-sided *P* value of .05 was considered the cutoff of statistical significance for all tests.

Table 1 Demographic and echocardiographic parameters at baseline and admission

Parameter	Young HV group (n = 106)	Adult HV group (n = 62)	<i>P</i>
Demographic data			
Age, y	10 ± 4	37 ± 15	<.001
Sex, male/female	57/49	39/23	.249*
Weight, kg	38.7 ± 18.7	73.3 ± 12.5	<.001
Height, m	1.43 ± 0.25	1.77 ± 10.48	<.001
BSA, m ²	1.24 ± 0.4	1.89 ± 0.21	<.001
BMI, kg/m ²	17.7 ± 3.4	23.2 ± 2.7	<.001
Heart rate, beats/min	75 ± 11	63 ± 11	<.001
Systolic BP, mm Hg	111 ± 12	122 ± 12	<.001
Systolic BP, percentile	73 ± 22		
Diastolic BP, mm Hg	62 ± 8	71 ± 10	<.001
Diastolic BP, percentile	54 ± 24		
Echocardiographic parameters			
IVSd, mm	6 ± 1	9 ± 2	<.001
IVSd, Z score	-0.48 ± 0.91		
LVEDD, mm	27 ± 4	31 ± 3	<.001
LVEDD, Z score	41 ± 6	47 ± 5	<.001
LVEDD, Z score	-0.29 ± 0.83		
LVEDV, mL	24 ± 11	40 ± 9	<.001
LVEDV, mL	63 ± 26	104 ± 22	<.001
LVEDV, Z score	-1.26 ± 0.87		
LVEF, % (Simpson)	63 ± 2	63 ± 4	.794
LVFS, % (M-mode)	34.4 ± 2.6	34.9 ± 4.5	.554
MV E wave, cm/sec	92 ± 11	77 ± 15	<.001
MV A wave, cm/sec	41 ± 8	47 ± 14	<.001
MV E/A ratio	2.3 ± 0.4	1.8 ± 0.7	<.001
E/e' ratio, average	5.8 ± 0.5	5.8 ± 1.6	.919
E-wave DT, msec	182.2 ± 29.5	198.9 ± 40.2	.007
IVRT, msec	63.9 ± 9.1	72.4 ± 13.8	<.001
GLS, %	-21.4 ± 1.2	-20.4 ± 1.7	<.001
SW velocity at MVC, m/sec	2.8 ± 0.3	3.5 ± 0.7	<.001

BMI, Body mass index; *BP*, blood pressure; *BSA*, body surface area; *HV*, healthy volunteer; *IVSd*, IVS diameter; *LVEDV*, LV end-diastolic volume; *LVEF*, LV ejection fraction; *LVEDD*, LV end-systolic diameter; *LVFS*, LV fractional shortening; *MV*, mitral valve.

Data are expressed mean ± SD or as numbers. *P* values were calculated using independent-samples *t* tests.

**P* value calculated using the χ^2 test.

RESULTS

Population Characteristics

Demographic and echocardiographic characteristics of our study population are summarized in Table 1. Among the 108 children and adolescents who were screened, two children were excluded (one was found to have fibroelastoma with mild aortic insufficiency, and the other had a depressed ejection fraction). A total of 106

healthy children and adolescents were eligible for analysis, with 22 children 2 to 6 years of age, 49 children 7 to 12 years of age, and 35 adolescents 13 to 18 years of age. We had 45 adult volunteers 19 to 40 years of age, nine 41 to 60 years of age, and eight 60 to 80 years of age.

Myocardial SWs in Children and Adolescents

In all young volunteers (≤ 18 years), natural SW propagation was easily detected and tracked along the IVS immediately after MVC from the base toward the apex. The mean propagation velocity of SWs across the IVS in the parasternal long-axis view was found to be 2.8 ± 0.3 m/sec (Table 1).

SW velocities correlated with demographic and echocardiographic parameters, as described in Table 2. We found a strong positive correlation with age ($r = 0.75$, $P < .001$; Figure 3A), a moderate correlation with SBP ($r = 0.54$, $P < .001$; Figure 4A), and a weak but significant correlation with GLS ($r = 0.33$, $P = .001$; Figure 5A), as well as with septal thickness ($r = 0.49$, $P < .001$; Figure 5A), and a moderate correlation with LVEDD ($r = 0.62$, $P < .001$; Figure 5B). Moderate correlations were also noted between SW velocities and conventional echocardiographic parameters of diastolic function—E-wave DT ($r = 0.58$, $P < .001$; Figure 6A) and mitral E/e' ratio ($r = 0.63$, $P < .001$; Figure 6B)—and a weak but significant correlation was found with IVRT ($r = 0.48$, $P < .001$; Figure 6C). Adjusting echocardiographic parameters using Z scores provided no significant correlations with SW velocities ($P > .05$ for all).

In a multivariate linear regression model (Table 2) age, mitral E/e' ratio, and GLS remained the only predictors of SW velocities after ad-

justing for hemodynamic (heart rate and SBP) and geometric (IVS thickness and LVEDD) parameters ($r = 0.81$).

Myocardial SW Findings in Adults Compared With Children

The mean SW velocity after MVC was significantly lower among healthy children and adolescents compared with adult volunteers (2.8 ± 0.3 vs 3.4 ± 0.8 , $P < .001$; Table 1). Combining measurements from both groups (all healthy volunteers 2-80 years of age), a strong positive correlation between SW velocities and age was found, persisting throughout life ($r = 0.73$, $P < .001$; Figure 3B).

Modeling of SW Velocities

Our theoretical wave propagation model predicted an increase in SW propagation speed with increasing wall thickness, despite constant material properties. For wall thicknesses of 5, 6, and 7 mm, the predicted SW propagation velocities were 2.2, 2.4, and 2.6 m/sec, respectively. The predicted speeds correspond very well with those observed in the age groups of 2 to 6, 7 to 12, and 13 to 18 years, which had comparable wall thicknesses. Furthermore, wall thicknesses of 4 and 10 mm were modeled and compared, which corresponded to the minimum and maximum values observed in the young volunteers (Figure 2B).

Feasibility and Reproducibility of SW Velocity Measurements

SWE was highly feasible in children and adolescents, so that SW velocities could be measured in all participants (100%). We

Table 2 Predictors of SW velocities among children and adolescents using univariate and multivariate analysis ($n = 106$)

Variable	SW velocities after MVC					
	Univariate		Multivariate		Collinearity diagnostics	
	<i>r</i>	<i>P</i>	β	<i>P</i>	Tolerance	VIF
Age	0.75	<.001	0.641	<.001	0.592	1.690
BSA	0.67	<.001				
BMI	0.41	<.001				
SBP	0.54	<.001				
HR	-0.24	.012				
Echocardiographic parameters						
Septal thickness	0.49	<.001				
LVEDD	0.62	<.001				
LVEDV	0.59	<.001				
LVEF (biplane Simpson)	-0.24	.012				
LVFS (M-mode)	0.08	.423				
GLS	0.33	.001	0.138	.041	0.784	1.276
E-wave DT	0.58	<.001				
E/e' ratio	0.63	<.001	0.297	<.001	0.804	1.244
IVRT	0.48	<.001				

BMI, Body mass index; BSA, body surface area; IVSd, IVS diameter; LVEDV, LV diastolic volume; LVEF, LV ejection fraction; LVFS, LV fractional shortening; SBP, systolic blood pressure; VIF, variance inflation factor.

In the univariate analysis, parameters in bold correlates significantly with SW velocities in children ($P < .05$). In the multivariate analysis, parameters in bold are significant predictors for SW velocities ($P < .05$).

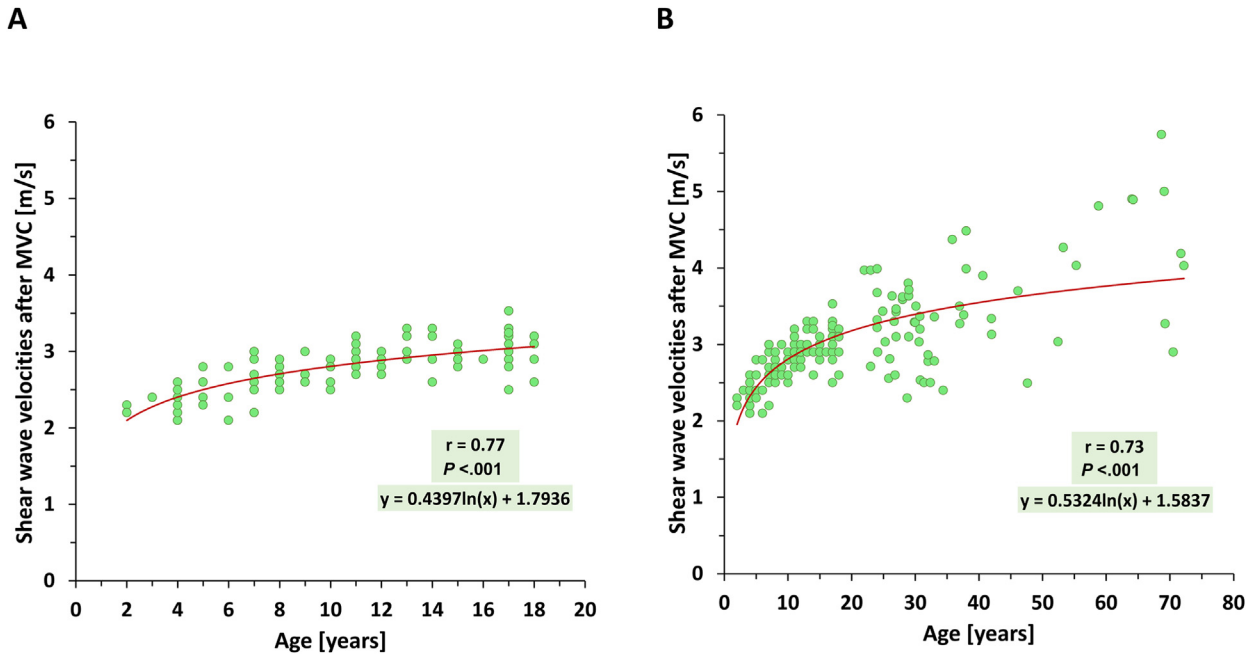


Figure 3 SW velocities and age. Correlation between velocities of natural SWs after MVC and age in **(A)** children and adolescents only ($n = 106$) and among **(B)** all healthy volunteers (children, adolescents, and adults [$n = 168$]). SW velocities show a significant strong positive dependence on age ($P < .001$). This increase was observed to be particularly steep in the first decade, while the curve flattened during adolescence and adulthood.

found a good to moderate slope estimator, intraobserver reproducibility, and test-retest reproducibility of our SW velocity estimates (ICC = 0.95 [95% CI, 0.90-0.97], ICC = 0.92 [95% CI, 0.84-0.96], and ICC = 0.83 [95% CI, 0.70-0.91], respectively). The interobserver variability was acceptable (ICC = 0.84; 95% CI, 0.70-0.92). Respective Bland-Altman plots are shown in [Figure 7](#).

DISCUSSION

The results of this study showed that the assessment of MS by means of HFR echocardiography-based measurements of propagation velocities of natural myocardial SWs after MVC in children and adolescents is feasible. Throughout the life span, natural SW velocities showed a clear dependence on age, verifying the need for age-

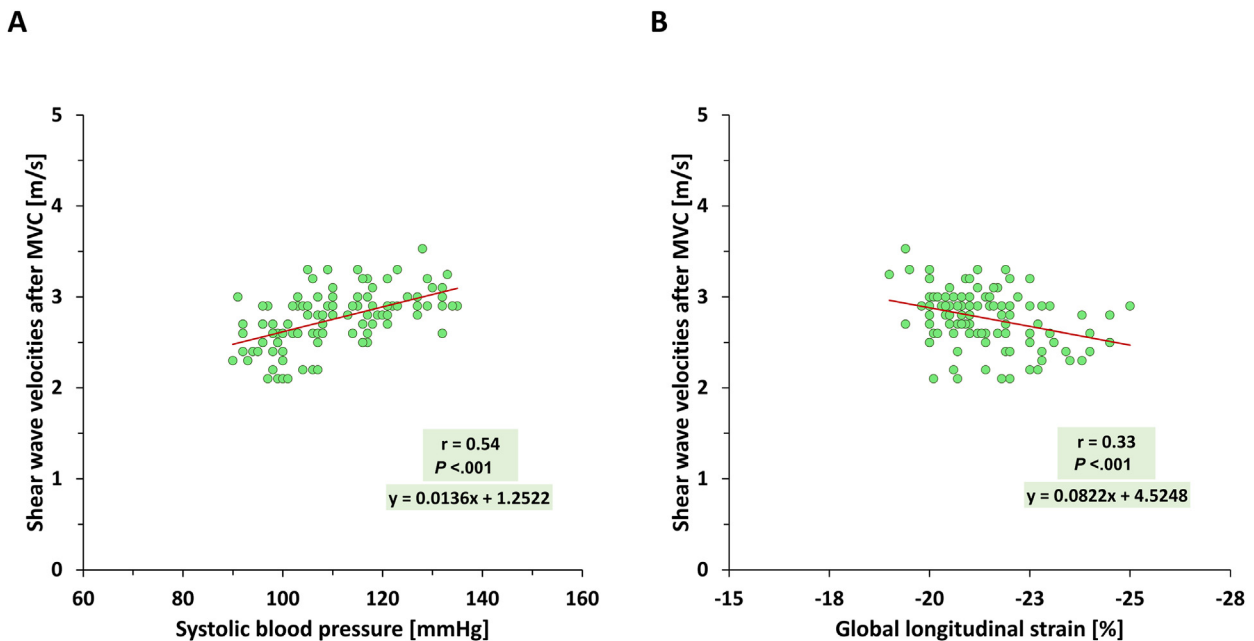


Figure 4 SW velocities and hemodynamic factors. A moderate positive correlation between SW velocities after MVC with SBP **(A)** and a negative weak correlation with GLS **(B)** were observed. In multivariate analysis, only GLS exhibited a weak correlation with SW velocities.

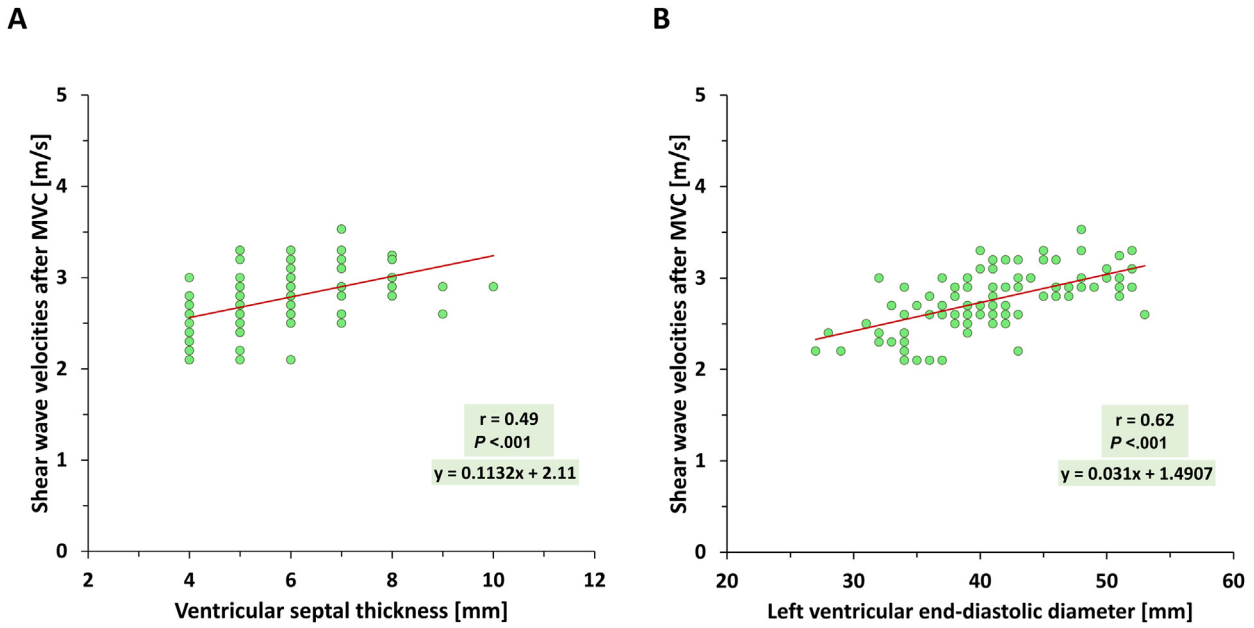


Figure 5 SW velocities and cardiac geometry. A weak positive correlation between SW velocities after MVC and IVS thickness was found among healthy children and adolescents **(A)**, and a moderate positive correlation was found with LVEDD **(B)**.

specific reference values. In addition, natural SW velocities correlated well with conventional parameters used to assess diastolic function. Modeling suggests that the particular increase in SW speed at a young age is due in part to the growth of the heart. To our knowledge, this is the first larger study to show the behavior of natural SW velocities from childhood into elderly and to provide a normal reference range for children (*Central Illustration*).

Induced vs Natural SWs

Echocardiographic SWE is a novel technique for the noninvasive assessment of MS.^{8,11,13,29} So far, only externally induced SW have been explored in children,^{22,23} while the behavior of natural SW velocities

has not yet been reported. In our study, natural SW velocities among healthy children and adolescents were higher than the externally induced SW that were explored by Malik *et al.*²³ using ARF. This might be because the externally induced SWs were measured strictly at end-diastole, depicting myocardial properties in a fully relaxed state, while the natural SWs are measured after MVC (i.e., at the beginning of the isovolumic contraction phase), when MS is already rising because of active contraction.^{11,14,16} Furthermore, the difference in excitation source (ARF vs valve closure) leads to distinct physical characteristics (e.g., wavelength and frequency) that play a significant role in how these waves interact with cardiac geometry affecting their propagation speed. Thereby, this could explain the variations between both waves velocities despite the consistent MS.^{11,14} However, when ARF-induced SW velocities were measured during the

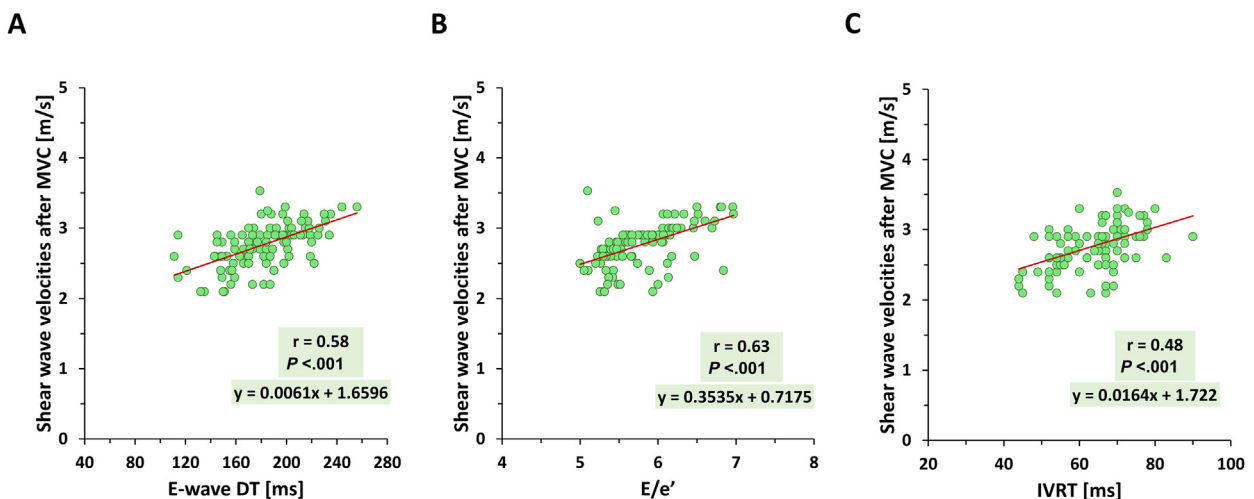


Figure 6 SW velocities and conventional parameters of diastolic function. **(A-C)** Conventional echocardiographic parameters for the assessment of diastolic function correlate significantly with natural SW velocities measured after MVC ($P < .001$).

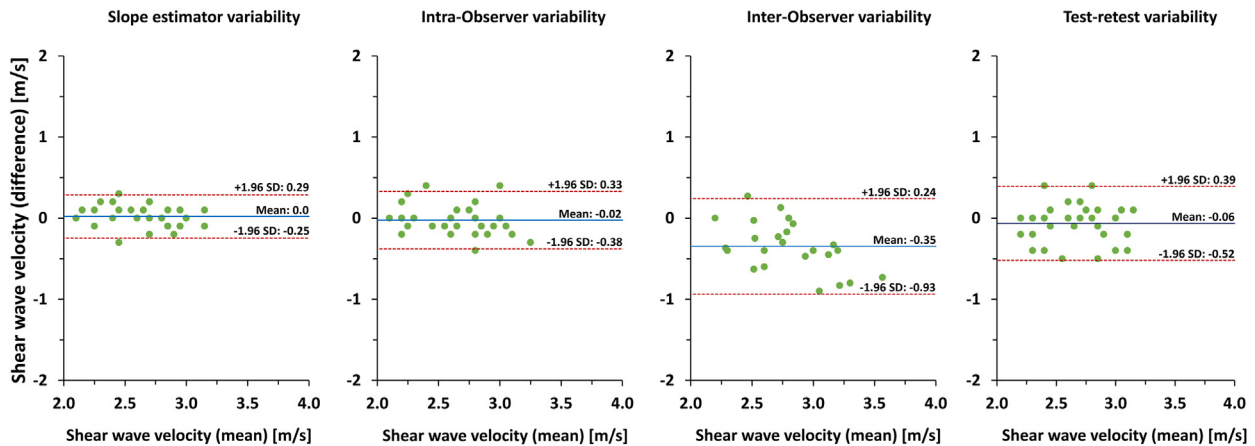


Figure 7 Bland-Altman plots for the reproducibility of SW velocity measurements. Variability of SW velocity measurements after MVC in children. Slope estimation and intraobserver and test-retest variability were assessed by A.Y. Interobserver variability was compared between A.Y. and L.W.

same time interval as for natural SWs (e.g., IVRT), Malik *et al.*¹⁵ found no statistically significant difference between both SW velocities among 20 healthy children.

Myocardial SW Velocities From Childhood Into Adulthood

SW velocities at MVC showed a clear dependency on age during childhood (Figure 3A) and adult life (Figure 3B), reflecting the natural evolution of MS with age. Our findings are in agreement with previous studies by Song *et al.*,²² who observed lower speeds of ARF-induced SWs among children compared with adults. Similar findings with ARF-induced SWs in healthy children and young adults (aged 1 month to 45 years) were reported by Malik *et al.*²³ and from a purely adult population (20-80 years of age) by Villemain *et al.*³⁰ These findings might reflect changes in MS due to a changing composition of extracellular matrix (changing ratio of collagen type I to collagen type III^{31,32}) that gets gradually stiffer with age.³³

Interestingly, our data revealed a strong positive logarithmic relationship between SW velocities and age, with a particularly steep increase in the first decade of life (Figure 3B). This might be explained by the rapid growth with significant increase in heart size and thickness during childhood.^{34,35} This adaptation occurs in response to the increased metabolic demands and hemodynamic changes, which cause a gradual stiffening of the cardiac matrix in an attempt to keep the wall stress normal.³⁵ Another possible explanation for such steepness is that septal thickening during early childhood might be associated with a diminished wave-guiding effect of the thinner walls on natural SWs, resulting in higher SW speeds that exceed the rate of age-related increase in MS.²³ Nevertheless, changes in cardiac geometry and local hemodynamics during growth might also alter leaflets dynamics, so that SWs with a different frequency spectrum and amplitude are generated. In theory, this might be a confounder potentially influencing propagation velocities even in the absence of true MS changes.^{11,14} Moving into adulthood, cardiac geometric maturation has been reached and stabilization of hemodynamics is achieved, so that changes of tissue properties (e.g., MS) are due mainly to accumulation of cross-linked collagen and fibrotic remodeling of the cardiac interstitium.³⁶ Our results indicate that age-specific reference values for SW speeds should be applied, and they are of particular importance in young children.

Influence of Myocardial Thickness on SW Velocities (Geometric Effects). In our study, we observed a significant positive correlation of SW velocities with increasing LVEDD and IVS thickness during childhood (Figure 5A). The guiding effect of a thinner septum in children could cause wave dispersion and result in underestimation of the wave speed. This suggests that the observed increase in SW speed might be partially attributed to the concurrent increase in wall thickness during growth.¹³ Our findings are also consistent with studies by Bézy *et al.*,^{16,37} Strachinaru *et al.*,²⁰ and Malik *et al.*,²³ who investigated variations of SW propagation velocity with myocardial septal thickness and muscle mass.

Our hypothesis is supported by our simulation model, which showed a clear increase in SW speed with increasing wall thickness (Figure 2) that resembles very well the observations in the young volunteers. Nevertheless, in the multivariate analysis model of our *in vivo* data, the effect of increasing IVS thickness on SW velocities was nonsignificant compared with the strong effect of age (Table 2), which might be explained by the collinearity of both parameters. This supports the hypothesis that the observed increase in SW velocities with age reflects changes in intrinsic myocardial properties more than the differences in wall thickness due to maintenance of wall stress within normal physiologic range during childhood.³⁸

Influence of Loading and Contractility on SW Velocities. Given that natural SWs occur at the beginning of the isovolumic contraction phase, we propose that both afterload and myocardial contractility (reflected by SBP and GLS) might theoretically influence natural SWs (Figure 4).¹³ However, considering the minor age-related changes in these parameters during childhood, it appears most plausible that natural SWs velocities primarily reflect age-related changes in MS. These thoughts are in line with findings from previous animal experiment by Bézy *et al.*¹⁶

Conventional Diastolic Parameters and Filling Pressure vs SW Velocities. In our study, we found moderate positive correlations between all conventional parameters of diastolic function and natural SW velocities after MVC among children and adolescents (Figure 6), except for IVRT, which showed a weak but significant correlation with SWs. Of note, all volunteers had normal cardiac function, leading to narrow ranges of all parameters of diastolic

function, suggesting that our observations reflect true lifelong changes in diastolic myocardial properties. When adjusted for geometric and hemodynamic effects in the multivariate model, mitral E-wave DT (as a marker of compliance) did not correlate with SW velocities, while E/e' ratio (as a central estimate of LV filling pressure) persisted as a predictor of SW velocity. A possible explanation could be that E-wave DT does not solely reflect LV stiffness but also LV relaxation, and thus different children might have indistinguishable DTs but significantly different LV stiffness if chamber relaxation is different.³⁹

Our findings are in agreement with those of a previous study by Bézy *et al.*,³⁷ who found a strong positive correlation between SW velocities after MVC and filling pressure assessed by E/e' ratio in healthy volunteers and patients with different cardiac diseases. Also in an animal experiment in pigs,¹⁶ acute increases in LV end-diastolic pressure were associated with a significant rise in SW speed after MVC. Moreover, we previously observed higher SW velocities in children with multisystem inflammatory syndrome after COVID-19 with elevated filling pressures compared with healthy children.²⁴ Another study by Petrescu *et al.*¹⁹ produced similar findings in adults with cardiac amyloidosis but not in healthy volunteers. We therefore assume that as children grow up, the insignificant growth-related increase in end-diastolic pressure weakly contributes to the observed rise in SW velocities ($\beta = 0.29$, $P < .001$), while age has the strongest effect.

Conversely, Malik *et al.*²³ did not find any correlation between the speed of ARF-induced SWs and mitral E/e' ratio. One possible explanation could be their small sample, with only 30 healthy children. In addition, ARF-induced SWs are of small magnitude with lower signal-to-noise ratio, which makes it more challenging to detect small differences in SW velocities. Also in other studies, ARF-based SWE showed negligible changes,^{17,40} whereas the velocities of natural SWs after MVC increased significantly with increasing end-diastolic pressure.⁴¹

Feasibility and Reproducibility of SW Velocities

In our study, we found that measuring naturally occurring SW was highly feasible in children and had good to moderate reproducibility (Figure 7). On the other hand, the variability of SW velocities among adults older than 40 years could be attributed to many factors. One possible explanation might be the better image quality and lower image depth in children, which offer a favorable signal-to-noise ratio and less variability in measurements among children. In addition, the higher SW values in adults are closer to the accuracy limits implied by the temporal resolution of our acquisitions, which results in higher measurement errors.^{18,19,42} Another possible explanation could be the true variability in MS due to the heterogeneous lifestyle among adults and elderly individuals, some of whom follow sedentary lifestyles and others more athletic lifestyles. However, to what extent physical exercise affects SW measurements is currently under investigation by our group.

Study Limitations

MS shows dynamic changes throughout the cardiac cycle, while the velocities of natural SWs after MVC reflect the myocardial state at the beginning of the isovolumic interval. Observed SWs might therefore be in part influenced by contractility or afterload and not entirely related to passive MS. Nevertheless, previous studies by our group^{16,21} could show that SW velocities after MVC are mainly and closely linked to passive end-diastolic MS.

CONCLUSION

Natural myocardial SW in children can be detected and quantified with a reasonable degree of reproducibility. Among children and adolescents, the velocities of these natural SWs show a clear and significant dependence on age and correlated well with parameters used to assess diastolic function. On the basis of our findings, natural SW measurements appear as a promising noninvasive tool for evaluating MS, which could help improve the comprehensive assessment of diastolic function. Establishing age-specific normal reference values is an important step to facilitate the use of natural SW imaging in future studies and to evaluate their clinical utility.

CONFLICTS OF INTEREST

None.

ACKNOWLEDGMENT

The authors thank Astrid Vloemans and Andrea Freys for their support.

REFERENCES

- Villemain O, Baranger J, Friedberg MK, et al. Ultrafast ultrasound imaging in pediatric and adult cardiology: techniques, applications, and perspectives. *JACC Cardiovasc Imaging* 2020;13:1771-91.
- Panesar DK, Burch M. Assessment of diastolic function in congenital heart disease. *Front Cardiovasc Med* 2017;4:5.
- Dragulescu A, Mertens L, Friedberg MK. Interpretation of left ventricular diastolic dysfunction in children with cardiomyopathy by echocardiography: problems and limitations. *Circ Cardiovasc Imaging* 2013;6:254-61.
- Nagueh SF. Left ventricular diastolic function: understanding pathophysiology, diagnosis, and prognosis with echocardiography. *JACC Cardiovasc Imaging* 2020;13:228-44.
- Nagueh SF, Smiseth OA, Appleton CP, et al. Recommendations for the evaluation of left ventricular diastolic function by echocardiography: an update from the American Society of Echocardiography and the European Association of Cardiovascular imaging. *J Am Soc Echocardiogr* 2016;29:277-314.
- Villemain O, Correia M, Khraiche D, et al. Myocardial stiffness assessment using shear wave imaging in pediatric hypertrophic cardiomyopathy. *JACC Cardiovasc Imaging* 2018;11:779-81.
- Gewillig M, Goldberg DJ. Failure of the fontan circulation. *Heart Failure Clin* 2014;10:105-16.
- Voigt JU. Direct stiffness measurements by echocardiography: does the search for the holy grail come to an end? *JACC Cardiovasc Imaging* 2019;12:1146-8.
- Petrescu A, D'hooge J, Voigt JU. Concepts and Applications of Ultrafast Cardiac Ultrasound Imaging. *Echocardiography (Mount Kisco, N.Y.)* 2020;38:7-15.
- Cikes M, Tong L, Sutherland GR, et al. Ultrafast Cardiac Ultrasound Imaging Technical Principles, Applications, and Clinical Benefits. *JACC Cardiovasc Imaging* 2014;7:812-23.
- Caenen A, Pernot M, Nightingale KR, et al. Assessing cardiac stiffness using ultrasound shear wave elastography. *Phys Med Biol* 2022;67.
- Villalobos Lizardi JC, Baranger J, Nguyen MB, et al. A guide for assessment of myocardial stiffness in health and disease. *Nat Cardiovasc Res* 2022;1:8-22.
- Caenen A, Bézy S, Pernot M, et al. Ultrasound shear wave elastography in cardiology. *JACC Cardiovasc Imaging* 2024;17:314-29.

14. Keijzer LBH, Caenen A, Voorneveld J, et al. A direct comparison of natural and acoustic-radiation-force-induced cardiac mechanical waves. *Sci Rep* 2020;10:18431.
15. Malik A, Villalobos Lizardi JC, Baranger J, et al. Comparison between acoustic radiation force-induced and natural wave velocities for myocardial stiffness assessment in hypertrophic cardiomyopathy. *JACC Cardiovasc Imaging* 2024;17:223-5.
16. Bézy S, Duchenne J, Orłowska M, et al. Impact of loading and myocardial mechanical properties on natural shear waves. *JACC Cardiovasc Imaging* 2022;15:2023-34.
17. Pernot M, Couade M, Mateo P, et al. Real-time assessment of myocardial contractility using shear wave imaging. *J Am Coll Cardiol* 2011;58:65-72.
18. Santos P, Petrescu AM, Pedrosa JP, et al. Natural shear wave imaging in the human heart: normal values, feasibility, and reproducibility. *IEEE Trans Ultrason Ferroelectr Freq Control* 2019;66:442-52.
19. Petrescu A, Santos P, Orłowska M, et al. Velocities of naturally occurring myocardial shear waves increase with age and in cardiac amyloidosis. *JACC Cardiovasc Imaging* 2019;12:2389-98.
20. Strachinaru M, Bosch JG, Schinkel AFL, et al. Local myocardial stiffness variations identified by high frame rate shear wave echocardiography. *Cardiovasc Ultrasound* 2020;18:40.
21. Petrescu A, Bézy S, Cvijic M, et al. Shear wave elastography using high-frame-rate imaging in the follow-up of heart transplantation recipients. *JACC Cardiovasc Imaging* 2020;13:2304-13.
22. Song P, Bi X, Mellema DC, et al. Pediatric cardiac shear wave elastography for quantitative assessment of myocardial stiffness: a pilot study in healthy controls. *Ultrasound Med Biol* 2016;42:1719-29.
23. Malik A, Baranger J, Nguyen MB, et al. Impact of ventricular geometric characteristics on myocardial stiffness assessment using shear-wave velocity in healthy children and young adults. *J Am Soc Echocardiogr* 2023;36:849-57.
24. Youssef AS, Salaets T, Bézy S, et al. Shear-wave elastography reflects myocardial stiffness changes in pediatric inflammatory syndrome post COVID-19. *JACC Cardiovasc Imaging* 2024;17:214-6.
25. Lopez L, Colan S, Stylianou M, et al. Relationship of echocardiographic Z scores adjusted for body surface area to age, sex, race, and ethnicity: the pediatric heart network normal echocardiogram database. *Circ Cardiovasc Imaging* 2017;10:e006979.
26. Rose JL. *Ultrasonic Guided Waves in Solid Media*. Cambridge: Cambridge University Press; 2014.
27. Kanai H. Propagation of spontaneously actuated pulsive vibration in human heart wall and in vivo viscoelasticity estimation. *IEEE Trans Ultrason Ferroelectr Freq Control* 2005 Nov;52:1931-42.
28. Finel V. Chapter 4: 3D Passive Elastography of the left ventricle. '3D ultrafast echocardiography: toward a quantitative imaging of the myocardium' Physics [physics]. PhD dissertation, Université Sorbonne Paris Cité, Paris. https://theses.hal.science/tel-02373882/file/FINEL_Victor_2_incomplete_20181115.pdf. Accessed November 21, 2019.
29. Sigrist RMS, Liao J, Kaffas A et, et al. Ultrasound elastography: review of techniques and clinical applications. *Theranostics* 2017;7:1303-29.
30. Villemain O, Correia M, Mousseaux E, et al. Myocardial stiffness evaluation using Noninvasive shear wave imaging in healthy and hypertrophic cardiomyopathic adults. *JACC Cardiovasc Imaging* 2019 Jul 1;12:1135-45.
31. Münch J, Abdelilah-Seyfried S. Sensing and responding of cardiomyocytes to changes of tissue stiffness in the diseased heart. *Front Cell Dev Biol* 2021;9:642840.
32. Marijjanowski MMH, van der Loos CM, Mohrschladt MF, et al. The neonatal heart has a relatively high content of total collagen and type I collagen, a condition that may explain the less compliant state. *J Am Coll Cardiol* 1994;23:1204-8.
33. Ward M, Iskratsch T. Mix and (mis-)match – the mechanosensing machinery in the changing environment of the developing, healthy adult and diseased heart. *Biochim Biophys Acta Mol Cell Res* 2020;1867:118436.
34. Bishop SP, Zhang J, Ye L. Cardiomyocyte proliferation from fetal-to adult-and from normal-to hypertrophy and failing hearts. *Biology* 2022;11:880.
35. Gaetani R, Zizzi EA, Deriu MA, et al. When stiffness matters: mechanosensing in heart development and disease. *Front Cell Dev Biol* 2020;8:334.
36. Biernacka A, Frangianni NG. Aging and cardiac fibrosis. *Aging Dis* 2011;2:158-73.
37. Bézy S, Cvijic M, Petrescu A, et al. Predictors of shear wave propagation speed assessed by shear wave elastography. *Eur Heart J* 2022;43(Supplement_2):ehac544.070.
38. Cvijic M, Bézy S, Petrescu A, et al. Interplay of cardiac remodelling and myocardial stiffness in hypertensive heart disease: a shear wave imaging study using high-frame rate echocardiography. *Eur Heart J Cardiovasc Imaging* 2020;21:664-72.
39. Shmuylovich L, Kovács SJ, Kovács SJ. E-wave deceleration time may not provide an accurate determination of LV chamber stiffness if LV relaxation/viscoelasticity is unknown. *Am J Physiol Heart Circ Physiol* 2007;292:2712-20.
40. Pislaru C, Urban MW, Pislaru SV, et al. Viscoelastic properties of normal and infarcted myocardium measured by a multifrequency shear wave method: comparison with pressure-segment length method. *Ultrasound Med Biol* 2014;40:1785-95.
41. Werner AE, Bezy S, Orłowska M, et al. Shear wave elastography: can we estimate filling pressures? *Eur Heart J* 2020;41(Supplement_2):ehaa946.1025.
42. Keijzer LBH, Strachinaru M, Bowen DJ, et al. Reproducibility of natural shear wave elastography measurements. *Ultrasound Med Biol* 2019;45:3172-85.